MRS Advances © 2017 Materials Research Society
DOI: 10.1557/adv.2017.30

Effect of Compound Dielectric and Metal Thinning on Metal-Insulator-Metal Resonant Absorbers for Multispectral Infrared Air-Bridge Bolometers

Robert E. Peale,[1] Seth Calhoun,[1] Chris J. Fredricksen,[1] Evan Smith,[2,3] Shiva Vangala,[2,4] Kevin Leedy,[2] Joshua R. Hendrickson,[2] and Justin W. Cleary[2]
[1]Department of Physics, University of Central Florida, Orlando FL 32816
[2]Air Force Research Laboratory, Sensors Directorate, Wright Patterson AFB, OH 45433
[3]KBRWyle Laboratories, Inc, Dayton, OH 45431
[4]Azimuth Corporation, Dayton, OH 45431

ABSTRACT

Addition of wavelength selective absorbers on microbolometers tends to increase their thermal mass and slow their infrared response times. Making the bolometric material an integral part of the absorber and minimizing layer thicknesses is one possible way to maintain high detector speeds. Here, we study experimentally the effect on permittivity of adding a layer of semiconducting VO_x between two layers of SiO_2. Additionally, we investigate theoretically the effect on resonance wavelength of thinning the metal in metal-insulator-metal plasmonic resonant absorbers.

INTRODUCTION

Our objective is the development of a high-speed high-sensitivity room-temperature bolometer array comprising individual pixels that are tailored to absorb within different specified wavelengths in the long-wave infrared (LWIR, 8-12 μm band) and mid-wave infrared (MWIR, 3-5 μm band). Applications include low noise night videography, high speed hot-target tracking, spectral sensing, and multi- or hyper-spectral imaging. Plasmonic perfect absorbers enable wavelength tunable absorption [1-5]. Our approach is integration of plasmonic perfect absorbers with room-temperature VO_x air-bridge bolometers to wavelength-selective sensitivity without degrading thermal time constant.

We recently described such bolometers, on top of which were placed plasmonic wavelength-selective absorbers [6]. The absorbers comprised a metal ground plane, a dielectric layer, and a patterned metal layer to form the well-known metal-insulator-metal (MIM) design. Fig. 1 presents a scanning electron microscope image of one of the bolometers [7]. Multispectral infrared detection was demonstrated for the Fig. 1 devices in [6,7]. The extra thermal mass of the absorber slowed the response time by 20% [7]. The remedy which we propose and investigate here is the possibility of integrating the bolometric VO_x layer inside the dielectric layer of the MIM, which would minimize the amount of dielectric in the structure, lowering thermal mass, and enhancing speed. A second remedy is to minimize the thicknesses of the metal ground plane and the patterned top metal. This paper investigates the effect of these design changes on the resonant absorption spectrum of the MIM absorber.

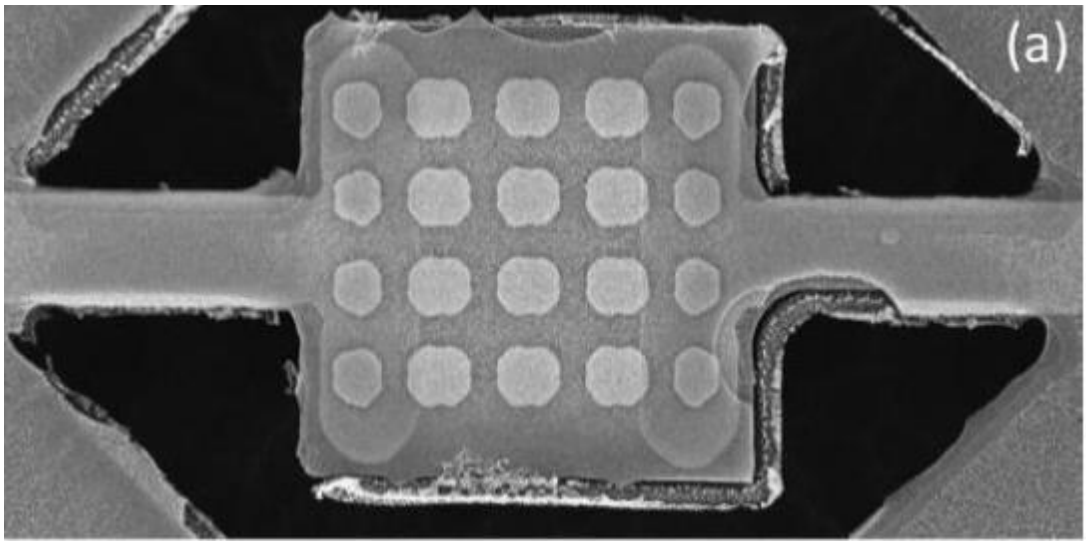

Fig. 1. Scanning electron microscope image of VO_x air-bridge bolometer with MIM plasmonic absorber patterned on top. The period of the array of gold squares is 7.5 μm, as accurately defined by the photomask used. From [7].

METHODS

Absorption resonances for the MIM structures are determined according to the model presented in Figure 2 [8]. Light incident with polarization perpendicular to the metal stripes of width *l*, i.e. in the plane of the figure with transverse magnetic field (TM), causes charges of opposite sign to appear the edges of the top metal. Corresponding image charges appear below the ground plane. These edge dipoles oscillate at the infrared frequency and are the source of the evanescent fields that propagate in the dielectric of thickness *t* under the stripe. Fields are well confined under each top metal pattern and do not interfere with fields of neighboring patterns until their separation is reduced to a quarter of their dimension *l* [8]. Thus, the absorption spectrum is due mainly to the geometry of the single unit cell (dimensions *l* and *t*) and the refractive index *n* of the dielectric. An array of stripes merely increases the fill factor and the total absorption [9]. Non-uniformity of the parameter *l*, as occurs near the edges of the actual device in Fig. 1, will broaden the resonance spectrum.

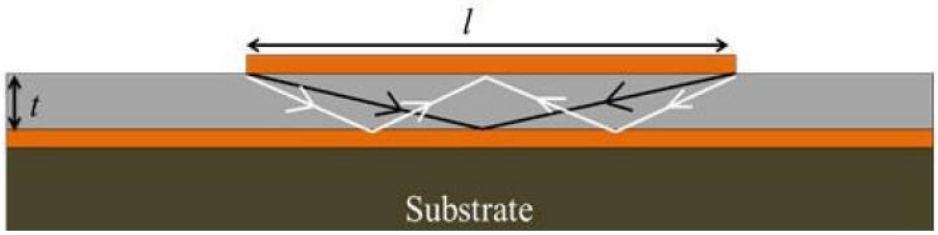

Figure 2. Schematic of MIM resonance model.

A standing wave model comprising oblique rays with an odd number of bounces *b* from the top and bottom metals well explains the resonant wavelengths [8], even though all dimensions are sub-wavelength so that ray optics should not apply. Shown in Fig. 2 are rays for $b = 1$ and 3. Resonances correspond to odd integer numbers of half-wavelengths along the indicated paths. For each value of *b*, there are a series of harmonics corresponding to values $m = 0,1,2,\ldots$ Equation 1 gives the resulting formula [8], which due to dispersion we solve graphically for the expected resonances.

https://doi.org/10.1557/adv.2017.30

$$\lambda(b,m) = \frac{2\,n(\lambda)}{b+2m}\sqrt{l^2 + (b+1)^2\,t^2} \quad . \qquad (1)$$

According to Equation 1, the resonances depend on only three experimental factors, namely the refractive index of the dielectric *n*, its thickness *t*, and the lateral dimension of the stripe *l*. This is not entirely supported by experiment, because it has been observed that when the top metals become optically thin, the resonances shift to shorter wavelength [10]. Part of this paper addresses this effect. Equation 1 also assumes that the dielectric is homogeneous, while our intent is to put a thin layer of semiconducting VO_x in the middle of it. If that insertion changes the index spectrum significantly, the resonances are expected to change. Thus, a first investigation was to determine the effect of the interlayer semiconductor on the effective refractive index of a $SiO_2/VO_x/SiO_2$ stack.

Layers were deposited and characterized in steps. The starting material was thermally-oxidized Si wafer. The thickness of the thermal oxide was manufacturer specified to be 1 µm. Amorphous vanadium oxide (VO_x, x≈2) with nominal thickness 100 nm was deposited by pulsed laser deposition at 550°C. Next, silicon dioxide was deposited by Plasma Enhanced Chemical Vapor Deposition (PECVD) for a nominal thickness of 650 nm.

Ellipsometry measurements were carried out using a Woolam IR-VASE ellipsometer. Ellipsometry data were collected over the spectral range of 1-15 µm on the starting wafer and after each subsequent material deposition. Optical constants were determined from these data at each step to confirm that the obtained constants for each layer are independent of the number of layers deposited. A model for each layer was fit to the ellipsometry data to obtain that layer's thickness and complex permittivity simultaneously. For SiO_2 and VO_x, the model featured Gaussian oscillator terms, and a Drude term was added for the VO_x only. The Gaussian terms are peak amplitude, energy and broadening, while the Drude terms are amplitude and energy. These terms specify the values of the imaginary part of the permittivity ε", and the calculation is Kramers-Kronig consistent. There is a real-part ε' offset that is fit, but this does not affect the value of ε". The WVASE software [11] fits the Gaussian terms, the Drude term, the ε' offset, and the thickness. These mathematical parameters are adjusted and fit until the model matches the raw ellipsometry data Psi and Delta.

Alternatively, when treating a $SiO_2/VOx/SiO_2$ stack as a single "effective" layer, we use a "point-to-point" fit method. Here the program simply attempts to match the index n and extinction κ spectra without developing an analytical model.

Electromagnetic simulations were performed to investigate what happens to the resonances when the top metal becomes optically thin. These were done using Lumerical FDTD software. Normally-incident plane waves were sourced multiple wavelengths away from the MIM surface, and the corresponding reflection was measured using a far-field monitor.

RESULTS AND DISCUSSION

The fit to the ellipsometry data confirmed the thickness of the thermal SiO_2 (1008 nm). The VO_x was found to have thickness 90 nm, which is 10% less than the nominal value. The fit gave 622 nm for the PECVD SiO_2, which is within 4% of the nominal value.

The refractive index and extinction coefficient spectra for a given layer determined from ellipsometry measured after each stage in the sequential deposition agree within a few percent.

https://doi.org/10.1557/adv.2017.30

The differences occur mainly at wavelengths beyond 12 μm. Thus, the statistical uncertainty in the optical constants is not more than a few percent.

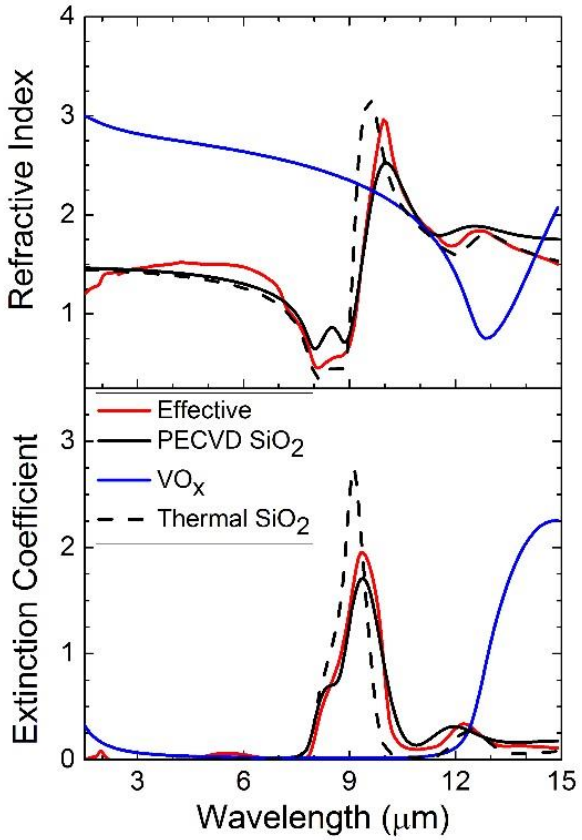

Figure 3. Refractive index and extinction coefficient spectra for $SiO_2/VO_x/SiO_2$ structure.

Figure 3 compares the optical constants for all layers individually with effective constants for the 3-layer stack as a whole. For the latter spectrum, the stack was considered as a single layer with a thickness of 1720 nm, which is the sum of the individual layer thicknesses. We first note that the spectra for thermal and PECVD oxide are somewhat different. The dispersion for the PECVD oxide appears somewhat lower, i.e. the index is not as high at its peak, and it is not as low at its minimum, while the peak extinction coefficient is only about two-thirds as strong. For the 9 μm Si-O stretch absorption band, there is a half micron difference in wavelength position for thermal and PECVD oxides. These differences in optical constants for thermal- and PECVD-SiO_2 can be attributed to the known higher density of the former and their slightly different stoichiometry [12].

Figure 3 shows that VO_x has less dispersion in the 8-12 μm LWIR region than does SiO_2, but the index still changes by a factor of 2.5 in this range. The effective constants of the stack as a whole are intermediate between those of thermal and PECVD SiO_2 alone with almost no signature of the VO_x interlayer. This can be attributed to the preponderance of SiO_2 in the structure (95%) and to that material's stronger dispersion.

Figure 4 presents the simulated resonances spectrum as a function of top metal (gold) thickness for the MIM structure. The dielectric (SiO_2) thickness t = 100 nm, with n = 1.357 and κ = 0. The stripe had width l = 2 μm. Thicknesses from 105 to 5 nm in steps of 5 nm were analyzed. The resonance position is almost independent of top metal thickness between 105 and

https://doi.org/10.1557/adv.2017.30

30 nm. Below 30 nm, the resonance weakens and shifts to *longer* wavelength by 9%. The direction of the shift is *opposite* what was observed experimentally [10]. This discrepancy is explained by a poor assumption made in the simulations, where it was assumed that the bulk values of the permittivity hold at all thicknesses. In reality, at 20 nm and below, the top metal films become discontinuous, and the bulk permittivity no longer applies [13]. When the effective permittivity values from [13] are used in the simulation, the wavelength blue shifts strongly in agreement with experiment, more than compensating for the red shift seen in Figure 4.

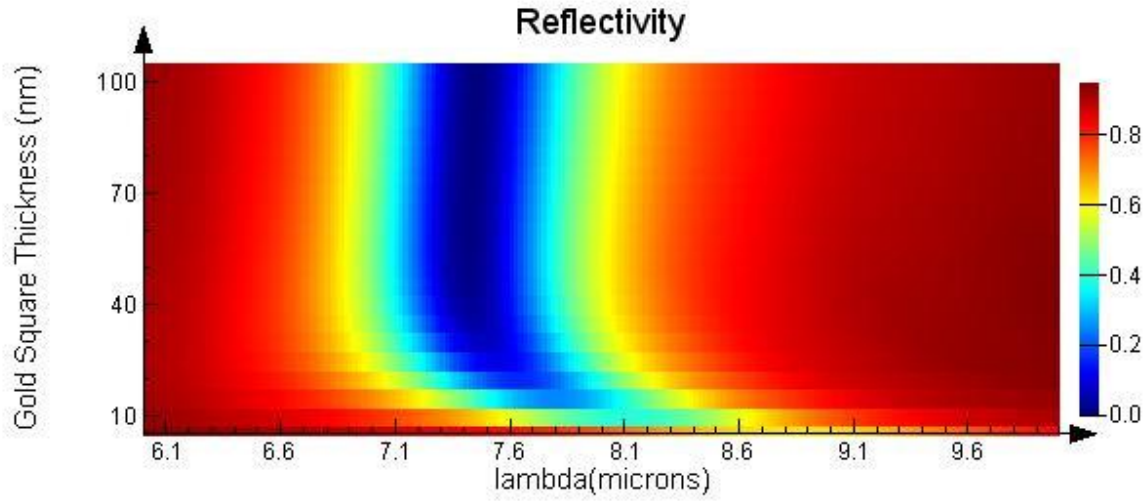

Figure 4. Simulated reflectance spectrum of MIM structure as function of top metal thickness with metal permittivity maintained at its bulk values.

CONCLUSIONS

The simple standing-wave MIM resonance design formula remains valid when a thin VO_x interlayer is present, with no effect on the refractive index of the insulator as a whole. On the other hand, when the metals used in the MIM structure become very thin, the resonances shift, showing that the model needs to be enhanced to include the effects of top metal thickness and permittivity.

ACKNOWLEDGMENTS

Authors acknowledge support from US Air Force Research Lab Contract Number FA8650-16-C-1738.

REFERENCES

1. Na Liu, Martin Mesch, Thomas Weiss, Mario Hentschel and Harald Giessen, “Infrared perfect absorber and its application as plasmonic sensor,” Nano Letters 10, 2342(2010).

2. Boyang Zhang, Joshua Hendrickson, and Junpeng Guo, "Multispectral near-perfect metamaterial absorbers using spatially multiplexed plasmon resonance metal square structures," J. Optical Soc. Am. B 30, 656 (2013).
3. Bingxin Zhang, Yanhui Zhao, Qingzhen Hao, Brian Kiraly, Iam-Choon Khoo, Shufen Chen, and Tony Jun Huang, "Polarization-independent dual-band infrared perfect absorber based on a metal-dielectric-metal elliptical nanodisk array," Optics Express 19, 15221 (2011).
4. Sang Jun Lee, Zahyun Ku, Ajit Barve, John Montoya, Woo-Yong Jang, S.R.J. Brueck, Mani Sundaram, Axel Reisinger, Sanjay Krishna & Sam Kyu Noh, "A monolithically integrated plasmonic infrared quantum dot camera," Nature Commun. 2, 286 (2011).
5. Yanxia Cui, Yingran He, Yi Jin, Fei Ding, Lui Yang, Yuqian Ye, Shoumin Zhong, Yinyue Lin, Sailing He, "Plasmonic and metamaterial structures as electromagnetic absorbers," Laser & Photonics Reviews 8, 495 (2014).
6. Evan M. Smith, Janardan Nath, James Ginn, Robert E. Peale, David Shelton, "Responsivity improvements for a vanadium oxide microbolometer using subwavelength resonant absorbers," Proc. SPIE 9819 – 50 (2016).
7. Evan M. Smith, Vanadium oxide microbolometers with patterned gold black or plasmonic resonant absorbers, PhD dissertation (University of Central Florida 2015).
8. Janardan Nath, Sushrut Modak, Imen Rezadad, Deep Panjwani, Farnood Rezaie, Justin W. Cleary, and Robert E. Peale, "Far-infrared absorber based on standing-wave resonances in metal-dielectric-metal cavity," Optics Express 23, 20366 (2015).
9. Janardan Nath, Deep Panjwani, Farnood Khalilzadeh-Rezaie, Mehmet Yesiltas, Evan M. Smith, James C. Ginn, David J. Shelton, Carol Hirschmugl, Justin W. Cleary, Robert E. Peale, "Infra-red spectral microscopy of standing-wave resonances in single metal-dielectric-metal thin-film cavity," Proc. SPIE 9544, 95442M (2015).
10. Janardan Nath, Douglas Maukonen, Evan Smith, Pedro Figueiredo, Guy Zummo, Deep Panjwani, Robert E. Peale, Glenn Boreman, Justin W. Cleary, Kurt Eyink, "Thin-film, wide-angle, design-tunable, selective absorber from near UV to far infrared," Proc. SPIE 8704 - 127 (2013).
11. JA Woolam, Co., www.jawoollam.com/ellipsometry-software/wvase.
12. Stanley Wolf and Richard N. Tauber, Silicon processing for the VLSI Era, Volume 1: Process Technology (Lattice, Sunset Beach CA, 1986) p 183.
13. Janardan Nath, Evan Smith, Douglas Maukonen, and Robert E. Peale, "Optical Salisbury screen with design-tunable resonant absorption bands," J. Appl. Phys. 115, 193103 (2014).

https://doi.org/10.1557/adv.2017.30